# Rigid Nanoscopic Containers for Highly Dispersed, Stable Metal and Bimetal Nanoparticles with Both Size and Site Control

**Chunlei Wang, Guangshan Zhu,* Jian Li, Xiaohui Cai, Yuhong Wei, Daliang Zhang, and Shilun Qiu*[a]**

**Abstract:** We demonstrate a novel strategy for the preparation of mesoporous silica-supported, highly dispersed, stable metal and bimetal nanoparticles with both size and site control. The supporting mesoporous silica, functionalized by polyaminoamine (PAMAM) dendrimers, is prepared by repeated Michael addition with methyl acrylates (MA) and amidation reaction with ethylenediamine (EDA), by using aminopropyl-functionalized mesoporous silica as the starting material. The encapsulation of metal nanoparticles within the dendrimer-propagated mesoporous silica is achieved by the chemical reduction of metal-salt-impregnated dendrimer–mesoporous silica by using aqueous hydrazine. The site control of the metal or bimetal nanoparticles is accomplished by the localization of inter- or intradendrimeric nanoparticles within the mesoporous silica tunnels. The size of the encapsulated nanoparticles is controlled by their confinement to the nanocavity of the dendrimer and the mesopore. For Cu and Pd, particles locate at the lining of mesoporous tunnels, and have diameters of less than 2.0 nm. For Pd/Pt, particles locate at the middle of mesoporous tunnels and have diameters in the range of 2.0–4.2 nm. The Pd and Pd/Pt nanoparticles are very stable in air, whereas the Cu nanoparticles are stable only in an inert atmosphere.

**Keywords:** dendrimers · mesoporous materials · metal ions · nanostructures · organic–inorganic hybrid composites

## Introduction

Great attention has been paid in recent years to solid-supported metal nanoparticles, due to their unique chemical and physical properties, such as small size and extremely large surface area, as well as their important applications in nanotechnology and heterogeneous catalysis.[1] Generally, control of the metal particle size is achieved by using preformed nanoparticles,[2] or the confined growth of nanoparticles within the void of porous materials, such as mesoporous silica.[3] The latter can be accomplished by adding the precursors directly to the synthesis gel,[4] by impregnation,[5] or by metal complex immobilization.[6] However, these methods have limited control over the size of the particles, due to the uncontrolled growth of the nanoparticles both inside the pores and on the external surface of the host.[4–6] Consequently, the ability to control precisely the sizes of nanoparticles when using porous host materials remains a great challenge.

An important goal in the investigation of catalysis is to develop synthetic approaches that achieve the accurate control of catalytic sites.[7] The structural homogeneity that arises from isolated single and uniformly distributed active sites (e.g., organic groups, metallic or bimetallic sites, nanoclusters, and nanoparticles) provides improved catalytic performance. Mesoporous silica-supported metal or bimetal nanoparticles have been extensively studied in recent years,[8] however, little effort has been devoted to tailoring the sites of the particles. This could be particularly attractive for the investigation of the structure-property relationships of the hybrid materials, and for the oriented growth of the nanostructures,[9] as well as for their application as artificial enzymes.[10]

Polyaminoamine (PAMAM) dendrimers[11] are cascade-branched macromolecules with fairly defined composition and structure, making them ideal candidates as hosts for metal nanoparticles.[12,13] Dendrimer branches can be used as selective gates to control the access of small molecules to

[a] Dr. C. Wang, G. Zhu, J. Li, X. Cai, Y. Wei, D. Zhang, Prof. S. Qiu
State Key Laboratory of Inorganic Synthesis and
Preparative Chemistry, Department of Chemistry, Jilin University
Changchun 130012 (China)
Fax: (+86) 431-516-8589
E-mail: zhugs@mail.jlu.edu.cn
sqiu@mail.jlu.edu.cn

 **DOI: 10.1002/chem.200500390**  

the encapsulated nanoparticles. Because metal particles are confined to the interior of the dendrimers, a large proportion of the surface is unpassivated, and can participate in the catalytic reaction. However, the dendrimer-encapsulated nanoparticles have poor mechanical and chemical stability and are difficult to separate.[14] Mesoporous silica,[15] with its highly regular structure, large surface area, as well as thermal and chemical stability, provides an excellent matrix for guest materials. However, as with other inorganic supports, the main drawback of mesoporous silica lies in the limited control over particle size and distribution in the ultimate catalyst. PAMAM-propagated porous silica, which combines the merits of both the dendrimer and the inorganic support, provides an ideal host for the preparation of a highly dispersed heterogeneous catalyst, in which the particle size and binding site of the nanoparticles are well controlled.[16]

Herein, we demonstrate a novel strategy for the preparation of mesoporous silica-supported stable metal and bimetal nanoparticles with both size and site control. PAMAM dendrons were grafted onto the surface of the tunnels of mesoporous silica, and metal or bimetal nanoparticles were then encapsulated by the dendrons (intra- or interdendrimer). The mesopores of the silica and the nanocavities of the dendrimer acted as a dual template for the control of the size of the metal or bimetal nanoparticles. The site control was achieved by dendrimers that were tethered onto the surface of the mesoporous tunnels. As a result, nanoparticles were located in either the middle or at the lining of the tunnels.

## Results and Discussion

PAMAM dendrimers ranging from half to four generations were propagated onto SBA-15 by modification of the literature methods and by using aminopropyl-functionalized mesoporous silica SBA-15 (AMP-SBA-15, 1.3 mmol per g of amine group per g of $SiO_2$) as starting material (G0-SBA-15).[17] For G*n*.5-SBA-15 ($n=0$–3), the amino propionates were formed by reacting preexisting amino groups with methyl acrylates (MA) through an aza-Michael-type addition in the presence of quaternary ammonium tetrabutyl ammonium bromide (TBAB) as catalyst.[18] Subsequently, the ester moieties were amidated by ethylenediamine (EDA) to complete the generation (G*n*-SBA-15, $n=1$–4). The desired generation of the dendrimer was produced by repeating these two steps. The grafting of the G4-PAMAM-dendron onto mesoporous silica is illustrated in Scheme 1.

Evidence for the successful grafting of the PAMAM dendron onto SBA-15 was obtained by performing FTIR spectroscopy, cross-polarized magic-angle spinning (CP-MAS) $^{13}$C NMR spectroscopy, and thermal gravimetric analysis (TGA). FTIR spectroscopy proved to be a very powerful technique to characterize the PAMAM dendrimers. The IR spectrum of aminopropyl-functionalized SBA-15 (Figure 1a) shows a band at 1640 cm$^{-1}$, which is characteristic of the amino group. All IR spectra of G*n*.5-propagated SBA-15 ($n=0$–3) (Figure 1b) exhibited a band at 1739 cm$^{-1}$, which was attributed to the formation of an ester group ($-COOCH_3$) by the Michael-type addition reaction of amino groups. Ester groups of G*n*.5-PAMAM-SBA-15 reacted with EDA to produce amides (−CONH−) and amino groups, which resulted in an increase in the intensity of the amide IR band (1540 cm$^{-1}$) and the disappearance of the ester group (1720 cm$^{-1}$) from the IR spectra of the G*n*-PAMAM-SBA-15 sample ($n=1$–4, Figure 1b). Weak ester bands were still present in the G1-PAMAM-SBA-15, indicating the incomplete amidation with EDA. Although IR spectra can provide evidence for whether the amidation reactions proceed to completion, they cannot show completion of the Michael addition reactions. CP-MAS $^{13}$C NMR spectroscopy was used to identify the functional groups of G4-PAMAM (Figure 1c). A representative spectrum of G4-PAMAM-SBA-15 shows a distinct peak at 173.84 ppm, which is attributed to the carbon residue of the amide group (−**C**ONH−). The peaks at 10.63, 22.15, and 32.57 ppm represent the original aminopropyl moiety, and the peak at 39.71 ppm is due to the carbon residue next to the amide group (−$CH_2$**C**$H_2$−CONH−). The broad peak at 49.61 ppm corresponds to the sum of the methylene carbon atoms attached directly to the nitrogen moiety (−N(**C**$H_2$C$H_2$CONH**C**$H_2$**C**$H_2$N)$_2$−). Thermal analysis data for G0 to G4-SBA-15 are summarized in Table 1. The weight loss for each generation was smaller than the theoretical value, indicating that the growth of the dendrimer on the mesoporous support was not complete.

Statistically, when using the divergent growth approach, only a small proportion of the higher generations of PAMAM dendrimers can be perfect. With the use of a solid support, the steric interference effect is pronounced, especially in nanosized tunnels of mesoporous silica. Bu et al.[19] investigated the structural defects of PAMAM-dendron-propagated silica gel. The structural defects were generated by cross-linking during amidation and the insufficient Michael addition of MA to diamine, which was hindered by steric crowding. The common method to achieve the PAMAM-dendron-propagated mesoporous silica or silica gel is time-consuming (4–10 days of reaction at 25–50 °C to complete a full generation). We found that quaternary ammonium salts are extraordinarily effective and useful catalysts for both Michael addition and amidation reactions during the preparation process; our modified method involving quaternary ammonium salt as catalyst requires only two days to complete each generation.[16]

The encapsulation of metal nanoparticles in dendrimer-propagated mesoporous silica was achieved by the chemical reduction of a metal-salt-impregnated dendrimer SBA-15 by using aqueous hydrazine, as demonstrated in Scheme 2. The small-angle X-ray diffraction (SAXRD) patterns of SBA-15, G4-SBA-15, and $Cu^0$-G4-SBA-15 (Figure 2a) showed three distinct peaks that can be indexed to the hexagonal *P6mm* space group. This result suggests that the mesoporous structure of SBA-15 has been retained after fourth-generation propagation of PAMAM, ion exchange, and reduction treatment. The wide-angle X-ray diffraction (WAXRD) patterns

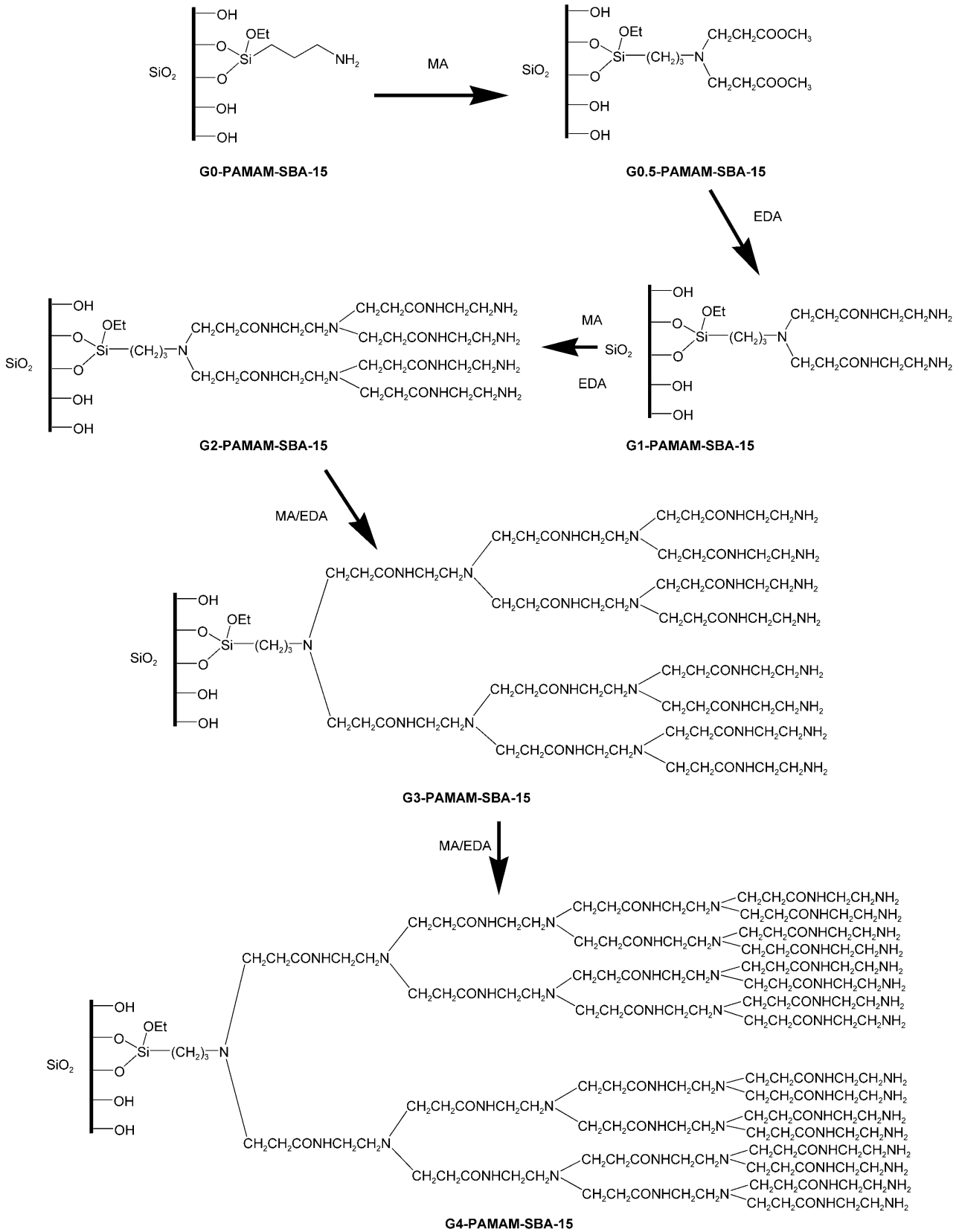


Scheme 1. Schematic illustration of the preparation of the G4-PAMAM-dendron-propagated mesoporous silica SBA-15, and the theoretical structure of G*n*-SBA-15.

  

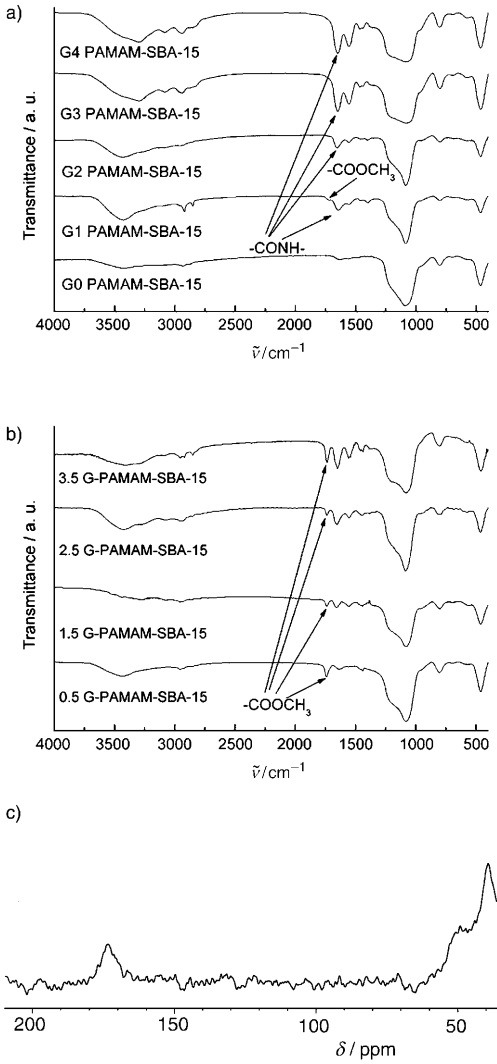


Figure 1. FTIR spectra showing a) the full-generation and b) the half-generation PAMAM-dendron-propagated mesoporous silica, demonstrating the stepwise synthesis by using a time-saving method with TBAB as catalyst. c) The CP-MAS $^{13}C$ NMR spectrum of G4-PAMAM-SBA-15.

Table 1. Amount of PAMAM dendron grafted onto SBA-15, determined by thermal gravimetric analysis (TGA).

| Generation[a] | Weight loss [%] | Grafted amount [mg g$^{-1}$ $SiO_2$][b] | Theoretical grafted amount [mg g$^{-1}$ $SiO_2$] |
|---|---|---|---|
| 0 | 7.5 | 8.1 | 8.1 |
| 1 | 19.4 | 241 | 399.8 |
| 2 | 28.6 | 401 | 1037.2 |
| 3 | 34.6 | 529 | 2326.1 |
| 4 | 45.5 | 836 | 4875.8 |

[a] Generation 0 refers to the aminopropyl-functionalized SBA-15. [b] Determined from the TGA weight-loss curves, weight loss% = (weight at 110 °C − weight at 700 °C)/weight at 700 °C.

of the $M^0$-G4-SBA-15 (M = Cu, Pd, Pd/Pt) did not show any distinct peak (Figure 2b), indicating that the $M^0$ nanoparticles encapsulated inside the fourth-generation PAMAM-propagated SBA-15 are very small.

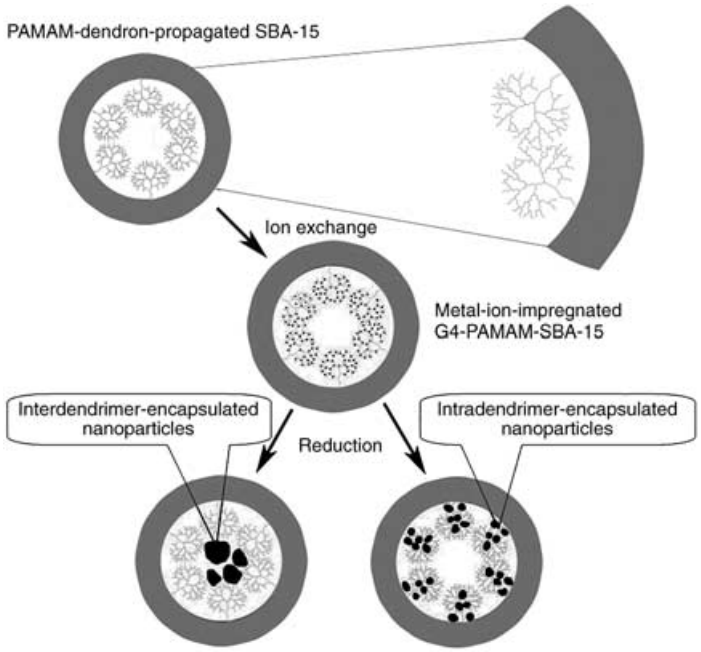


Scheme 2. Representation of the procedure used for the preparation of G4-SBA-15-encapsulated metal or bimetal nanoparticles, and their theoretical structure.

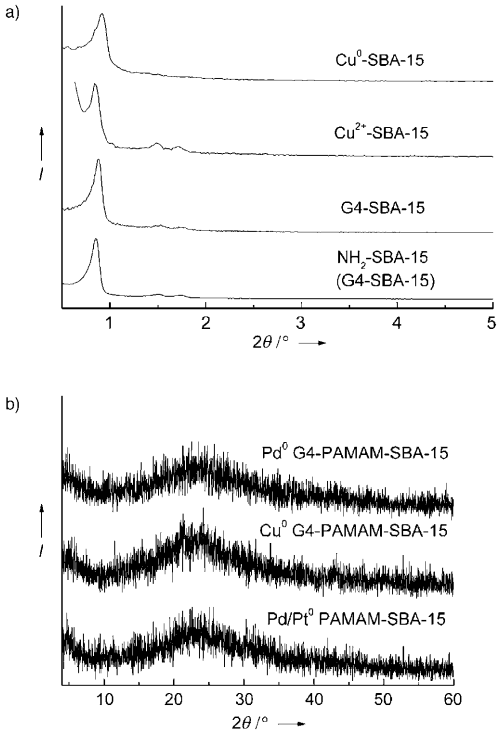


Figure 2. a) Small-angle XRD patterns for $NH_2$-SBA-15 (G0-SBA-15), G4-SBA-15, $Cu^{2+}$-G4-SBA-15, and $Cu^0$-G4-SBA-15. b) Wide-angle XRD patterns for $Cu^0$-G4-SBA-15, $Pd^0$-G4-SBA-15, and $Pd/Pt^0$-G4-SBA-15.

Figure 3a shows representative UV/Vis spectra for the G4-SBA-15, $Cu^{2+}$ ion-exchanged fourth-generation PAMAM-propagated SBA-15 ($Cu^{2+}$-G4-SBA-15), $Cu^0$-G4-

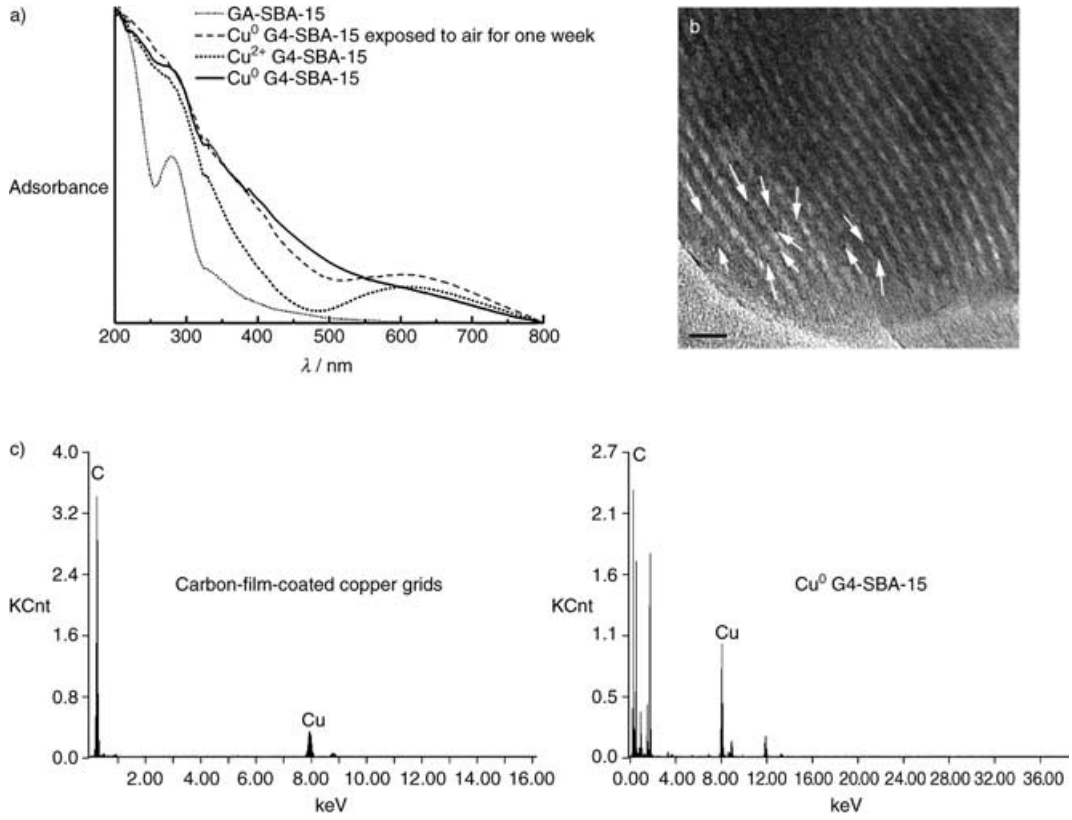


Figure 3. a) UV/Vis absorption curves for G4-SBA-15, $Cu^{2+}$-G4-SBA-15, $Cu^{0}$-G4-SBA-15, and $Cu^{0}$-G4-SBA-15 after exposure to air for one week; b) TEM image of the $Cu^{0}$ nanoparticles in G4-SBA-15 (scale bar = 20 nm); c) comparison of EDX spectra of carbon film and the $Cu^{0}$-G4-SBA-15 sample.

SBA-15, and $Cu^{0}$-G4-SBA-15 after exposure to air for one week. The G4-SBA-15 spectrum showed a band centered at 270 nm. $Cu^{2+}$-G4-SBA-15 exhibited a strong d–d transition of $Cu^{2+}$ with a peak center at 590 nm. After reduction by aqueous hydrazine, the adsorption band originating at 590 nm disappeared and was substituted by a spectrum increasing almost exponentially toward shorter wavelengths. This result implies that the reduced Cu inside the nanocontainer of PAMAM dendrons exists as clusters rather than as isolated atoms.[12b] A plasmon resonance band was not observed in the absorption spectra of $Cu^{0}$-G4-SBA-15, which indicates that the Cu nanoclusters are smaller than 5 nm.[20] The Cu cluster encapsulated in PAMAM-propagated SBA-15 was very stable in an inert atmosphere, as shown by the results of UV/Vis spectroscopy performed for up to 10 days. However, after exposure to air for one week, the Cu clusters reverted to intradendrimer $Cu^{2+}$ ions, as indicated by the reappearance of the band at 590 nm (Figure 3a). High-resolution transmission electron microscopy (HRTEM) provides direct evidence for the control at the atomic level of the sites of the nanoparticles. Figure 3b shows that the Cu clusters are of uniform size (< 2.0 nm), and are highly dispersed in G4-SBA-15. Most of the nanoparticles are located at the lining of the tunnels of the mesoporous silica, indicating that the nanoparticles are intradendrimeric. Despite the presence of defects in the dendron-propagated SBA-15, the encapsulated nanoparticles retain their shape and size, as do the individual dendrimers, after reduction of $Cu^{2+}$-G4-SBA-15 by hydrazine. Energy-dispersive X-ray spectra (EDX) of the carbon-film-coated copper grids, which were used in the EDX sample preparation, showed the Cu content to be $2.2 \pm 0.4$ mol % (average value taken over several large regions), whereas in the $Cu^{0}$-G4-SBA-15 sample regions, the Cu content was $7.0 \pm 0.6$ mol % (Figure 3c). This result confirms the presence of copper in the sample PAMAM-dendron-grafted mesoporous silica.

The representative UV/Vis spectra of G4-SBA-15, $Pd^{2+}$-G4-SBA-15, and $Pd^{0}$-G4-SBA-15 are shown in Figure 4a. The absorption peak at 280 nm of $Pd^{2+}$-G4-SBA-15, which was attributed to a ligand-to-metal charge-transfer (LMCT) transition, disappeared after reduction by hydrazine. HRTEM images of $Pd^{0}$-G4-SBA-15 (Figure 4b and c) clearly show how the nanoparticles are roughly spherical and nearly monodispersed, with diameters less than 2.0 nm. Notably, most of them were encapsulated intradendrimerically at the lining of the tunnels, with only a small fraction encapsulated interdendrimerically in the middle of the tunnels (indicated by the white arrow in Figure 4b).

The UV/Vis spectra of G4-SBA-15, $Pd^{2+}$/$Pt^{2+}$-G4-SBA-15, and Pd/$Pt^{0}$-G4-SBA-15 (Figure 5a) show results similar to those for Pd. However, HRTEM images (Figure 5b and c) show that, in contrast to the Pd nanoparticles, most of the

  

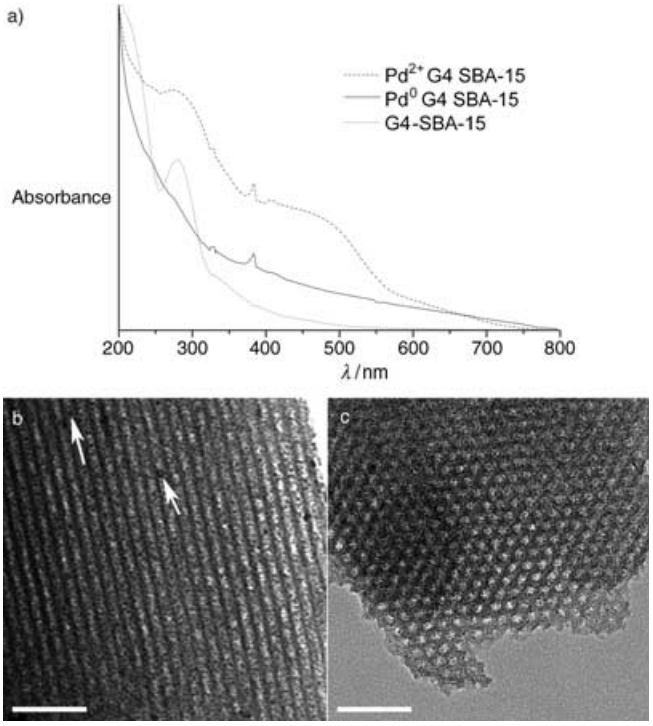


Figure 4. a) UV/Vis absorption curves for G4-SBA-15, $Pd^{2+}$-G4-SBA-15, and $Pd^0$-G4-SBA-15. b) and c) TEM images of the $Pd^0$ nanoparticles in G4-SBA-15. Each scale bar represents 50 nm.

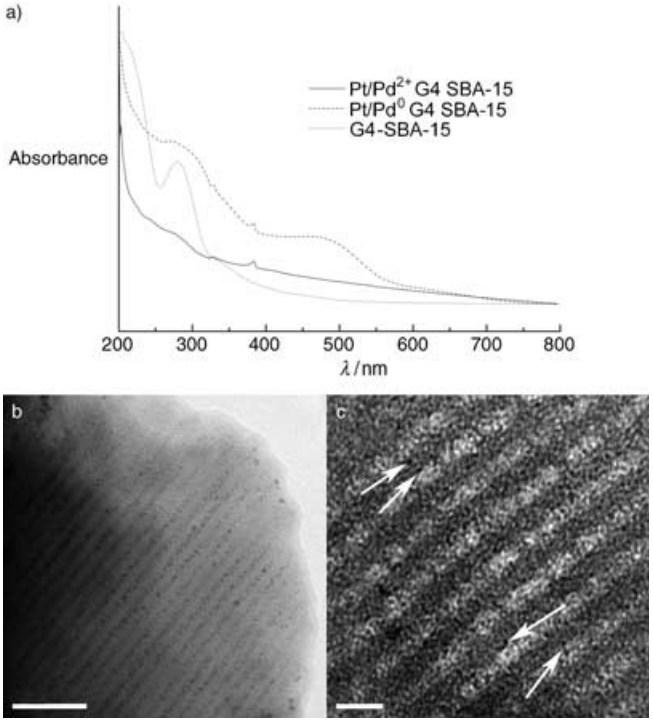


Figure 5. a) UV/Vis absorption curves for G4-SBA-15, Pd/$Pt^{2+}$-G4-SBA-15, and Pd/$Pt^0$-G4-SBA-15. b) and c) TEM images of the Pd/$Pt^0$ bimetal nanoparticles in G4-SBA-15. The scale bars in (b) and (c) represent 50 nm and 10 nm, respectively.

Pd/Pt bimetal nanoparticles were encapsulated interdendrimerically in the middle of the mesoporous silica tunnels and were of irregular shape, with diameters ranging from 2.0 to 4.2 nm. A small fraction of the Pd/Pt nanoparticles with diameter $< 2.0$ nm were encapsulated intradendrimerically at the brim of the tunnels (Figure 5c, indicated by the white arrows). These results indicate that the Pd/Pt bimetal particle sizes were insensitive to the stabilizer (PAMAM dendrimer), due to the introduction of Pt. Because the interactions between the Pt nanoparticles and the PAMAM dendrimer are weaker than for the Pd nanoparticles, more dendrimers are required to stabilize the Pd/Pt alloy nanoparticles than the Pd nanoparticles.[12j,k,13c] The complexation behavior of $Pt^{2+}$ with interior tertiary amines is much slower than that of $Pd^{2+}$. The $Pt^{2+}$/$Pd^{2+}$-G4-SBA-15 solution was stirred for only one day before reduction with aqueous hydrazine, so that most $Pt^{2+}$ ions and some of the $Pd^{2+}$ ions were complexed with (or only adsorbed onto) the periphery amine groups and not the interior tertiary amines. As a result, the Pd/Pt bimetal nanoparticles were formed on the exterior of the dendrimers after reduction.

Results of EDX spectroscopic analysis of $Pd^0$-G4-SBA-15 and Pd/$Pt^0$-G4-SBA-15 are shown in Figure 6. The distinct Pd signal of the $Pd^0$-G4-SBA-15 sample is seen in Figure 6a. The EDX spectrum of the Pd/Pt-G4-SBA-15 gave a Pd/Pt atom ratio of about 4 (Figure 6b). Highly dispersed Ag and Pt nanoparticles were not achieved by using this method, possibly due to the weak interaction between the dendri-

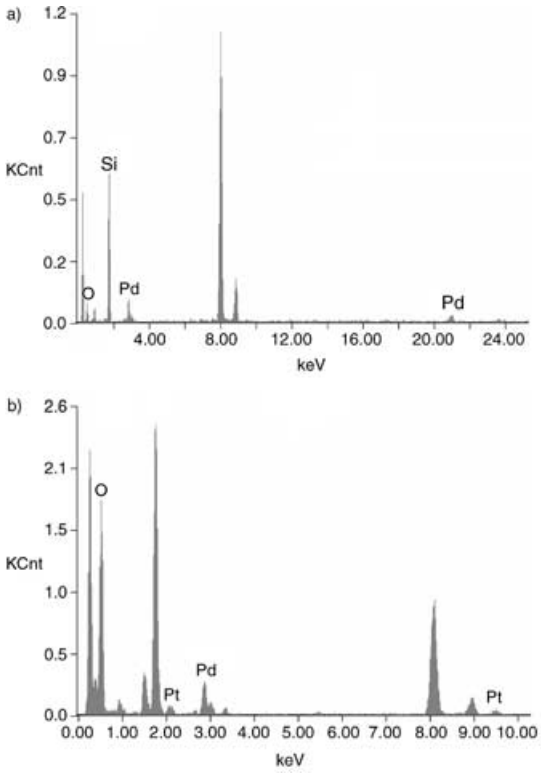


Figure 6. EDX spectra of a) $Pd^0$-G4-SBA-15 and b) Pd/$Pt^0$-G4-SBA-15.

mers and the nanoparticles. Both Pd and Pd/Pt nanoparticles encapsulated by the G4-PAMAM-SBA-15 were stable in air for one month without aggregation.

For comparison, blank mesoporous silica SBA-15 was used to accommodate Pd and Pd/Pt nanoparticles under the same conditions. The loading amount of the metal nanoparticles in the blank SBA-15 is much lower than that in G4-SBA-15, due to the absence of the complexation metal ions of the PAMAM dendrons and the rediffusion of metal ions in solution during reduction with aqueous hydrazine. Figure 7a and b show the TEM images of Pd nanoparticles in the tunnels of blank SBA-15. Pd nanoparticles that are larger than the mesopore diameter are observed outside the mesopores (black arrows), due to the reduction of metal ions diffused in solution. The size distribution of the nanoparticles is not uniform, and they are larger than 2 nm, due to the uncontrolled growth of the particles. TEM images for Pd/Pt nanoparticles accommodated in SBA-15 are shown in Figure 7c and d. Some nanoparticles are adsorbed onto the external surface, however, several areas without any particles are also observed (Figure 7c, marked regions). The result of microarea elemental analysis (by EDX) indicates that the Pd/Pt atom ratio is not homogeneous, in contrast to that for $Pd/Pt^0$-G4-SBA-15.

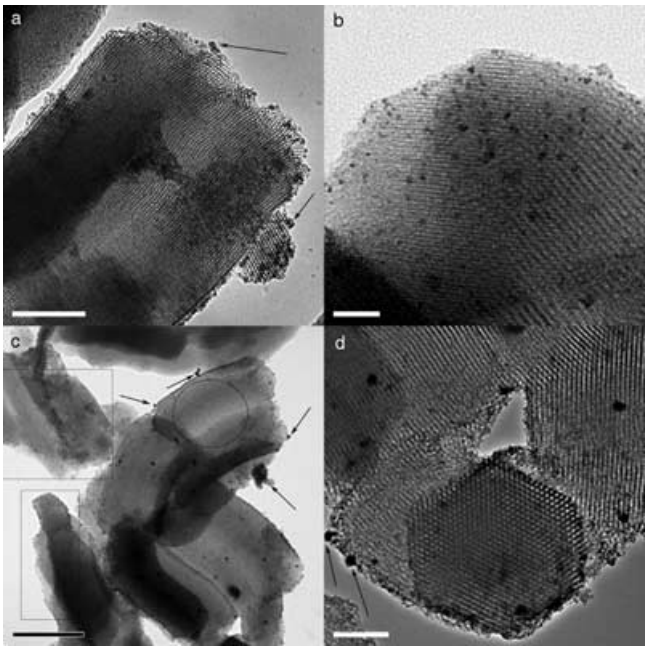


Figure 7. TEM images of Pd nanoparticles (a and b) and Pd/Pt bimetal nanoparticles (c and d) in blank SBA-15. The scale bars represent 200 nm (a), 50 nm (b), 0.5 μm (c), and 100 nm (d).

In conclusion, we have demonstrated a method for preparing highly dispersed, stable metal (Cu and Pd) and bimetal (Pd/Pt) nanoparticles on a solid support by using PAMAM dendrons as stabilizers. Fairly monodispersed metal nanoparticles were confined to the nanocavities of dendrimers or were encapsulated by external dendrimers. The sites of the nanoparticles, which located close to the walls or in the middle of the tunnels, were controlled by the formation of either intra- or interdendrimerically-encapsulated nanoparticles. These hybrid materials provide an ideal means to investigate structure-property relationships in heterogeneous catalysis.

## Experimental Section

**Synthesis of PAMAM-dendron-propagated mesoporous silica SBA-15**: In a typical synthesis, 1 g of aminopropyl-functionalized mesoporous silica (1.3 mmol $g^{-1}$ silica, prepared according to the literature[17]) was dispersed in MeOH (50 mL). Catalyst TBAB (tetrabutyl ammonium bromide, 10 mol %) was added to this suspension, then methyl acrylate (MA, 56 mL) was added under stirring. The mixture was refluxed for 24 h under nitrogen. The solid was then filtered, washed with MeOH (3 × 30 mL) and dichloromethane (3 × 30 mL), and dried at 40 °C in a vacuum.

The full-generation PAMAM-SBA-15 was prepared as follows: 1 g of the half-generation PAMAM-SBA-15 was added to ethylenediamine (200 mL) in methanol (100 mL), with TBAB as catalyst. The mixture was stirred at 70 °C under nitrogen for 1 day. The solid was filtered, washed with MeOH (3 × 30 mL) and dichloromethane (3 × 30 mL), and dried at 40 °C in a vacuum.

**General method for the preparation of metal or bimetal nanoparticles encapsulated within dendrimer-propagated SBA-15**: G4-SBA-15 (0.1 g) was added to 250 mL of a freshly prepared aqueous solution (16 mM) of a metal salt or a mixture of metal salts. The mixture was stirred for 24 h at room temperature, then the powder was filtered and washed thoroughly. The products were defined as $M^{2+}$-G4-SBA-15 (M = Cu, Pd, Pd/Pt). The resulting $M^{2+}$-G4-SBA-15 was redispersed in deionized water (50 mL), and aqueous hydrazine was added dropwise (0.4 mL). The resulting suspension was stirred for 2 h. The solid was then filtered, washed with water (3 × 50 mL), and dried in a vacuum. The product $M^0$-G4-SBA-15 was stored in an inert atmosphere. Pd and Pd/Pt nanoparticles incorporated in blank mesoporous silica SBA-15 were prepared under the same conditions.

**Characterization**: The IR spectra were recorded by using a Bruker 66V FTIR spectrometer in the range of 400–4000 $cm^{-1}$ using the KBr disk method. The UV/Vis diffuse reflectance spectra were obtained by using a Perkin–Elmer Lambda 20 spectrometer. Powder X-ray diffraction was recorded by using a Siemens D5005 diffractometer with $Cu_{K\alpha}$ radiation ($\lambda = 1.5406$ Å) at 35 kV and 30 mA. Thermal gravimetric analysis (TGA) was performed by using a Perkin–Elmer TGA-7 instrument with a heating rate of 20 °C $min^{-1}$ in air. Transmission electron microscopy (TEM) experiments were performed by using a JEM 3010 electron microscope (JEOL, Japan) with an acceleration voltage of 300 kV. Energy-dispersive X-ray spectroscopy (EDX) analysis was performed by using an EDAX PHOENIX 30T.

## Acknowledgements

This work was supported by the National Natural Science Foundation of China (Grant No. 29873017 and 20101004), and the State Basic Research Project (G2000077507).

[1] a) G. Schmid, *Nanoscale Materials in Chemistry* (Ed.: K. J. Klabunde), Wiley, New York, **2001**, p.15; b) R. Schlogl, S. B. Abd Hamid, *Angew. Chem.* **2004**, *116*, 1656; *Angew. Chem. Int. Ed.* **2004**, *43*, 1628, and references therein.

[2] a) H. Bönnemann, R. M. Richards, *Eur. J. Inorg. Chem.* **2001**, *10*, 2455; b) C. L. Bianchi, S. Biella, Gervasini, L. Prati, M. Rossi,

  

*Catal. Lett.* **2003**, *85*, 91; c) R. M. Rioux, H. Song, J. D. Hoetelmeyer, P. Yang, G. A. Somorjai, *J. Phys. Chem. B* **2005**, *109*, 2192.

[3] a) Z. Konya, V. F. Puntes, I. Kiricsi, J. Zhu, J. W. Ager III, M. K. Ko, H. Frei, P. Alivisatos, G. A. Somorjai, *Chem. Mater.* **2003**, *15*, 1242; b) I. Yuranov, P. Moeckli, E. Suvorova, P. Buffat, L. Kiwi-Minsker, A. Renken, *J. Mol. Catal. A* **2003**, *192*, 239; c) J. Gu, J. Shi, L. Xiong, H. Chen, M. Ruan, *Microporous Mesoporous Mater.* **2004**, *74*, 199.

[4] a) U. Junges, W. Jaxobs, I. Voigt-Martin, B. Krutzsch, F. Schüth, *J. Chem. Soc. Chem. Commun.* **1995**, 2283; b) M. Hartmann, C. Bischof, Z. Luan, L. Kevan, *Microporous Mesoporous Mater.* **2001**, *44/45*, 385.

[5] a) C. M. Yang, H. S. Sheu, K. J. Chao, *Adv. Funct. Mater.* **2002**, *12*, 143; b) Y. J. Han, J. M. Kim, G. D. Stucky, *Chem. Mater.* **2000**, *12*, 2068; c) K. B. Lee, S. M. Lee, J. Cheon, *Adv. Mater.* **2001**, *13*, 517; d) Y. Plyuto, J.-M. Berquer, C. Jacquiod, C. Ricolleau, *Chem. Commun.* **1999**, 1653; e) Q.-H. Xia, K. Hidajat, S. Kai, *Catal. Today* **2001**, *68*, 255; f) C. H. Ko, R. Ryoo, *Chem. Commun.* **1996**, 2467.

[6] a) P. Mukherjee, C. R. Patra, R. Kumar, M. Sastry, *PhysChemComm* **2001**, *5*, 1; b) A. Fukuoka, N. Higashimoto, Y. Sakamoto, M. Sasaki, N. Sugimoto, S. Inagaki, Y. Fukushmao, M. Ichikawa, *Catal. Today* **2001**, *66*, 23; c) Y. Guari, K. Soulantica, C. Thieuleux, A. Mehdi, C. Reyé, B. Chaudret, R. J. P. Corriu, *New J. Chem.* **2003**, *27*, 1029.

[7] a) D. E. De Vos, M. Dams, B. F. Sels, P. A. Jacobs, *Chem. Rev.* **2002**, *102*, 3615; b) K. L. Fujdala, T. D. Tilley, *J. Catal.* **2003**, *216*, 265; c) J. M. Thomas, *Top. Catal.* **2001**, *15*, 85.

[8] a) J. P. M. Niederer, A. B. J. Arnold, W. F. Hölderich, B. Spliethof, B. Tesche, M. Reetz, H. Bönnemann, *Top. Catal.* **2002**, *18*, 265; b) J. M. Thomas, R. Raja, B. F. G. Johnson, T. J. O'Connell, G. Sankar, T. Khimyak, *Chem. Commun.* **2003**, 1126.

[9] a) For a recent review, see: Y. Xia, P. Yang, Y. Sun, Y. Wu, B. Mayers, B. Gates, Y. Yin, F. Kim, H. Yan, *Adv. Mater.* **2003**, *15*, 353; b) Z. Zhang, B. Wei, G. Ramanth, P. M. Ajayan, *Appl. Phys. Lett.* **2002**, *77*, 3764; c) H. Ago, K. Marata, M. Yumura, J. Yotani, S. Uemura, *Appl. Phys. Lett.* **2003**, *82*, 811.

[10] a) N. Toshima, *Supramol. Sci.* **1998**, *5*, 395; b) Y. Murakami, J. Kikuchi, Y. Hisaeda, O. Hayashida, *Chem. Rev.* **1996**, *96*, 721.

[11] a) E. Buhleier, W. Wehner, F. Vogtle, *Synthesis* **1978**, 155; b) A. W. Bosman, H. M. Janssen, E. W. Meijer, *Chem. Rev.* **1999**, *99*, 1665; c) D. A. Tomalia, A. M. Naylor, W. A. Goddard III, *Angew. Chem.* **1990**, *102*, 119; *Angew. Chem. Int. Ed. Engl.* **1990**, *29*, 138; d) D. A. Tomalia, H. D. Durst, *Top. Curr. Chem.* **1993**, *165*, 193.

[12] a) R. M. Crooks, M. Zhao, L. Sun, V. Chechik, L. K. Yeung, *Acc. Chem. Res.* **2001**, *34*, 181; b) M. Zhao, L. Sun, R. M. Crooks, *J. Am. Chem. Soc.* **1998**, *120*, 4877; c) M. Zhao, R. M. Crooks, *Angew. Chem.* **1999**, *111*, 375; *Angew. Chem. Int. Ed.* **1999**, *38*, 364; d) M. Zhao, R. M. Crooks, *Adv. Mater.* **1999**, *11*, 217; e) M. Zhao, R. M. Crooks, *Chem. Mater.* **1999**, *11*, 3379; f) L. K. Yeung, R. M. Crooks, *Nano Lett.* **2001**, *1*, 14; g) V. Chechik, R. M. Crooks, *J. Am. Chem. Soc.* **2000**, *122*, 1243; h) Y. Niu, L. K. Yeung, R. M. Crooks, *J. Am. Chem. Soc.* **2001**, *123*, 6840; i) L. Sun, R. M. Crooks, *Langmuir* **2002**, *18*, 8231; j) R. W. Scott, A. K. Datye, R. M. Crooks, *J. Am. Chem. Soc.* **2003**, *125*, 3708; k) Y. M. Chung, H. K. Rhee, *Catal. Lett.* **2003**, *85*, 159.

[13] a) E. H. Rahim, F. S. Kamounah, J. Frederiksen, J. B. Christensen, *Nano Lett.* **2001**, *1*, 499; b) A. Henglein, *J. Phys. Chem. B* **2000**, *104*, 2201; c) K. Esumi, A. Suzuki, A. Yamahira, K. Torigoe, *Langmuir* **2000**, *16*, 2604; d) K. Esumi, R. Isono, T. Yoshimura, *Langmuir* **2004**, *20*, 237; e) R. Narqayanan, M. A. El-Sayed, *J. Phys. Chem. B* **2004**, *108*, 8572; f) L. Yang, Y. Luo, X. Jia, Y. Ji, L. You, Q. Zhou, Y. Wei, *J. Phys. Chem. B* **2004**, *108*, 1176; g) D. Liu, J. Gao, C. J. Murphy, C. T. Williams, *J. Phys. Chem. B* **2004**, *108*, 12911; h) J. Zheng, M. S. Stevenson, R. S. Hikida, P. G. V. Patten, *J. Phys. Chem. B* **2002**, *106*, 1252.

[14] "Catalysis by Metals and Alloys": V. Ponec, G. C. Bond, *Stud. Surf. Sci. Catal.* **1995**, *95*, 1.

[15] D. Zhao, Q. Huo, F. Jiang, B. F. Chmelka, G. D. Stucky, *J. Am. Chem. Soc.* **1998**, *120*, 6024.

[16] a) S. C. Bourque, H. Alper, L. E. Manzer, P. Arya, *J. Am. Chem. Soc.* **2000**, *122*, 956; b) S. C. Bourque, F. Maltais, W. J. Xiao, O. Tardif, H. Alper, P. Arya, L. E. Manzer, *J. Am. Chem. Soc.* **1999**, *121*, 3035; c) S. Antebi, P. Arya, L. E. Manzer, H. Alper, *J. Org. Chem.* **2002**, *67*, 6623; d) J. P. K. Reynhardt, H. Alper, *J. Org. Chem.* **2003**, *68*, 8353; e) P. Arya, G. Panda, N. V. Rao, H. Alper, S. C. Manzer, *J. Am. Chem. Soc.* **2001**, *123*, 2889; f) S. M. Lu, H. Alper, *J. Am. Chem. Soc.* **2003**, *125*, 13126.

[17] a) R. J. P. Corriu, E. Lancelle-Beltran, A. Mehdi, C. Reyé, S. Brandès, R. Guilard, *J. Mater. Chem.* **2002**, *12*, 1355; b) A. Stein, B. J. Melde, R. C. Schorden, *Adv. Mater.* **2000**, *12*, 1403.

[18] a) T. C. Wabnitz, J. Yu, J. B. Spencer, *Chem. Eur. J.* **2004**, *10*, 484; b) L. Xu, J. Li, S. Zhou, C. Xia, *New J. Chem.* **2004**, *28*, 183.

[19] a) J. Bu, R. Li, C. W. Quah, K. J. Carpenter, *Macromolecules* **2004**, *37*, 6687; b) J. P. K. Reynhardt, Y. Yang, A. Sayri, H. Alper, *Chem. Mater.* **2004**, *16*, 4095.

[20] a) H. Abe, K.-P. Charle, B. Teshce, W. Schulze, *Chem. Phys.* **1982**, *68*, 137; b) A. C. Curtis, D. G. Duff, P. P. Edwards, D. A. Jefferson, B. F. G. Johnson, A. I. Firkland, A. S. Wallace, *Angew. Chem.* **1988**, *100*, 1543; *Angew. Chem. Int. Ed. Engl.* **1988**, *27*, 1530.

Received: February 22, 2005
Published online: June 23, 2005